2018 European Control Conference (ECC)
June 12-15, 2018. Limassol, Cyprus

Supervised Energy Management in Advanced Aircraft Applications

Alberto Cavallo[1], Giacomo Canciello[1] and Antonio Russo[1]

***Abstract*— A control strategy is proposed for energy management onboard the innovative More Electric Aircraft (MEA) concept. The objective is to reduce generator sizing (and weight onboard) by using battery packs as extra-energy sources. The flow of energy is regulated by a Buck-Boost Converter Unit (BBCU), suitably driven. The controller is composed of a two-layers architecture, where the bottom layer is devoted to current-tracking purposes, while the upper level takes care of the safe switching between the different control objectives. Rigorous stability tools are presented for both controllers, based on the Theory of Sliding Mode Control and of Common Lyapunov Functions. Detailed simulation with switching power electronic components show the effectiveness of the proposed approach.**

***Index Terms*— Aerospace applications; Sliding Mode Control; Switched Systems.**

I. INTRODUCTION

The interest of the aeronautic factories towards the More Electric Aircraft (MEA) is continuously growing in the last two decades. MEA concept essentially has the objective to replace as far as possible hydraulic and pneumatic devices with their electric counterpart. There are many reasons for this increasing interest [1]. First, the flexibility in use and the good reliability electric devices have when compared to hydraulic and/or pneumatic counterparts. For example, replacing hydraulic actuators for the aircraft control surfaces with electromechanical (EMA) or electrohydrostatic (EHA) actuators [2], results in weight reduction, as the whole central hydraulic system can be removed, increased reliability, since a local fault has just a local effect and does not propagates along the actuators' supply pipe, and increased efficiency, typical of electric motors wrt their hydraulic counterpart. Moreover, energy-saving techniques specific of electric motors, e.g., regenerative breaking, can be considered in order to reduce energy consumption [3], [4].

As a corollary to this approach, it is clear that increased use of electric energy on aircraft has consequences on new ideas for management, generation and distribution of electric power onboard. In particular, devices like batteries come into play with more sophisticated tasks than the usual role of "energy-reserve" in the event of complete generator fault. However, in the traditional approach, basically most of the management tasks are left to the humans (pilot and/or crew), while it is clear that a more sophisticated and articulated energy management approach requires large use of automated control strategies. This, in turn, calls for rigorous stability proofs of the control algorithms and strategies, since no human override can be expected to ensure a correct behaviour in unforeseen circumstances.

The application addressed in this paper is the use of the battery pack (or supercapacitors [5]) onboard as an autonomous device able to help the main current generator in the case of overload. The framework is the classic dual DC busses aeronautic energy distribution system, with a 270VDC bus [6] supplied by the aircraft generator (usually, a three-phase generator undergoing a rectification), and a 28VDC bus [7], where the battery pack resides. As a bridge between the two busses, a bidirectional DC-DC converter can be used [8], [9]. The idea of using the battery as a device to support the generator when extra-power is required due to an overload event has been proposed in [10], [11]. This idea needs two levels of control: a low-level, aimed at precisely tracking current and voltage references [8], and a high-level supervisor, switching among different control modes in such a way that stability is ensured [10], [12]. Note that the solution proposed in the above papers considers just an asymptotic (actually, exponential) approach to the desired setpoint. On the contrary, in this paper we propose a different implementation of the same strategy, able to reach the setpoints in finite time and to still guarantee stability of the switching supervisor. The key point is to use a First-Order Sliding Mode (FOSM) control [13], then estimating the finite reaching time for each mode. Since the so-called *reduced order system* (i.e., the system dynamics remaining after the system has reached the sliding manifold, as discussed later) is linear, the stability among switching modes can be solved rigorously as an LMI (Linear Matrix Inequality) problem, or using any CLF (Common Lyapunov Functions) approach.

A simulation campaign performed with a MATLAB/Simulink/SimPowerSystem detailed simulator show the effectiveness of the proposed control strategy.

II. BBCU MODEL

As mentioned in the Introduction, the key element in the automatic energy management of the energy onboard is the BBCU. This device acts as a bridge between HV and LV sides, and its action defines the energy flow from and to the battery. The basic schematic of the BBCU is shown in Figure 1, with R_D representing a generic resistive load, as usual in the literature when the active power consumption is to be considered. In order to deduce the dynamic model of the BBCU, define a binary control variable $u : \mathbb{R} \to \{0, 1\}$ and let $u = 1$ refer to the configuration (Q_1 on, Q_2 off) and $u = 0$ to (Q_1 off, Q_2 on). Then the equations of the

[1]Alberto Cavallo, Giacomo Canciello and Antonio Russo are with Dept. of Engineering, University of Campania "L. Vanvitelli", 81031, Aversa, Italy {alberto.cavallo, giacomo.canciello, antonio.russo1}@unicampania.it

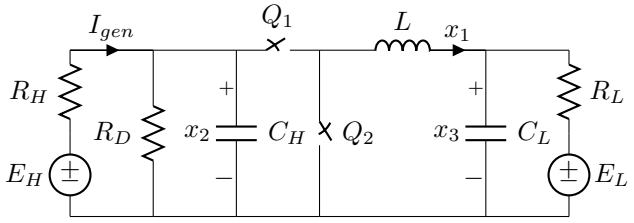

Fig. 1: Bidirectional converter schematic

converter are

$$\dot{x}_1 = -\frac{1}{L}x_3 + \frac{1}{L}x_2 u, \tag{1}$$

$$\dot{x}_2 = -\alpha x_2 - \frac{1}{C_H}x_1 u + \beta_H, \tag{2}$$

$$\dot{x}_3 = \frac{1}{C_L}x_1 - \frac{1}{R_L C_L}x_3 + \beta_L, \tag{3}$$

$$y = x_1, \tag{4}$$

where x_1 is the current flowing through the inductor L, x_2 is the voltage on the capacitor C_H on the high-voltage bus side, x_3 is the voltage on the capacitor C_L on the low-voltage bus side and

$$\alpha = \left(\frac{1}{R_H} + \frac{1}{R_D}\right)\frac{1}{C_H}, \tag{5}$$

$$\beta_i = \frac{E_i}{R_i C_i},\ i \in [H, L]. \tag{6}$$

In the phase of battery charging, we will assume that a (possibly constant) current reference is considered. The aim of the low-level controller in this phase is to force the inductor current to track this current reference. For this reason, in (4) the output is the current x_1.

The other task of the low-level controller is to limit the generator current. For this purpose we must express this quantity as

$$I_{gen} = \frac{E_H - x_2}{R_H}. \tag{7}$$

Then, if an upper bound I_{OL} is selected for I_{gen}, then (7) with $I_{gen} = I_{OL}$ translates into a reference value $\bar{x}_2$ for x_2.

III. Control Design

The proposed control law is based on the selection of a sliding manifold presented in [10]. Specifically, the sliding manifold is defined based on the control objective, so that as long as the controlled system state belongs to the manifold, the control objective is achieved. The low-level control proposed in [10] was based on a High-Gain control strategy and a modification of the sliding manifold for the controlled system. Specifically, in order to avoid initial control peaks, the state was assumed to belong to the sliding surface since the initial time instant, and this requires the manifold to be "bent" initially. This assumption requires perfect knowledge of the initial conditions of the system. In this paper we remove the assumption of knowledge of the initial conditions, since in some cases it may be unrealistic. As a result, this prevents us from using high-gain strategies, and we resort to the classic VSC (Variable Structure Control) approach. Different control objectives are considered, and the related sliding manifold derived. Next, a supervisor is in charge for scheduling the different control actions. However, in order to keep stability, care must be taken when switching among different sliding surfaces. For this issue, we exploit the well-known property of classic VSC to reach the sliding manifold in finite time. By computing an estimate of this time, rigorous stability conditions can be imposed at the supervisory control taking care of the switching.

A. Low-level control

As stated before, the basic control objective is to regulate either the current flowing in the inductor or voltage of the HV capacitor through a sliding mode control. Define a sliding manifold

$$\mathcal{S} = \{(y, x_2) | \sigma(y, x_2) = 0, \forall t \geq 0\} \tag{8}$$

where the sliding function σ is

$$\sigma(y, x_2) = k x_2 - y \tag{9}$$

and k is a scalar constant to be chosen. In [10] it has been shown that differentiating once the function σ the control u explicitly appears, hence a First-Order Sliding Mode can be enforced if the so-called *equivalent control* u_{eq}, obtained by solving for u the algebraic equation $\dot{\sigma} = 0$, satisfies the condition [14]

$$0 < u_{eq} < 1. \tag{10}$$

Moreover, by choosing [10]

$$k = \frac{E_H \pm \sqrt{E_H^2 - 4\alpha R_H^2 C_H \bar{y}\left(R_L \bar{y} + E_L\right)}}{2R_H\left(R_L \bar{y} + E_L\right)} \tag{11}$$

in sliding mode the output of the system tracks the reference variable $\bar{y}$. The following Theorem defines the control law such that the sliding mode is accomplished.

Theorem 1: Consider the system (1)–(4), and the sliding function (9), where k is defined in (11). Assume that k satisfies

$$-\frac{E_L}{E_H R_L}\left(1 + \frac{R_H}{R_D}\right) < k < \frac{E_H - E_L\left(1 + \frac{R_H}{R_D}\right)}{R_L E_H + R_H E_L} \tag{12}$$

and is such that (10) is fulfilled. Then, the control law

$$u = \begin{cases} 0 & \text{when } \sigma \leq 0 \\ 1 & \text{when } \sigma > 0 \end{cases} \tag{13}$$

guarantees that the sliding manifold (8) is reached in finite time, and the closed-loop system converges to a stable equilibrium point.

Proof: Starting with the reaching phase, consider first the initial case $\sigma(0) < 0$, which yields the control input $u = 0$. In this case it is easy to show that the system (1)–(3) converges exponentially to a point such that, due to (12), σ is positive. Analogously, starting with $\sigma > 0$ and considering $u = 1$, it is possible to prove that, due to (12), σ exponentially converges to a negative value. Thus, in both cases the

surface $\sigma = 0$ must be reached in finite time, and this ends the reaching phase.

The second part of the proof, the stability in sliding mode, is easily derived from [10, Theorem 1]. Essentially, after replacing the equivalent control in (1)–(3), the reduced order system is

$$\dot{z} = Az + Bw \tag{14}$$

where $z = [x_{20} \quad x_{30}]^T$, the subscript '0' referring to the variable evolution restricted to the sliding manifold, $w = [E_H \quad E_L]^T$ and

$$A = \begin{bmatrix} -\frac{\alpha C_H}{Lk^2+C_H} & -\frac{k}{Lk^2+C_H} \\ \frac{k}{C_L} & -\frac{1}{R_L C_L} \end{bmatrix}, \tag{15}$$

$$B = \begin{bmatrix} \frac{1}{R_H(Lk^2+C_H)} & 0 \\ 0 & \frac{1}{R_L C_L} \end{bmatrix}. \tag{16}$$

It is clear that the reduced-order system has an exponentially stable steady-state. ∎

We have just shown that the system reaches the sliding manifold in finite time. An estimate of the reaching time can be computed as follows. Preliminarily, we give the following Lemma.

Lemma 1: Consider the LTI system

$$\dot{x} = Ax + \xi, \quad x(0) = x_0, \tag{17}$$

$$y = c^T x \tag{18}$$

where $x \in \mathbb{R}^n$, $A \in \mathbb{R}^{n \times n}$ is a Hurwitz matrix and $c, \xi \in \mathbb{R}^n$ are constant vectors. Assume that

$$\lim_{t \to \infty} y(0)y(t) < 0 \tag{19}$$

so that there exists a finite $\hat{t}(x_0)$ such that $y(\hat{t}(x_0)) = 0$. Then for x_0 in a ball of radius ρ, centred at the origin, an estimate of the largest (as x_0 varies) time $\hat{t}$ is

$$\hat{t} = \frac{1}{|\gamma + \epsilon|} \log \left[\left(\frac{2M}{\epsilon} \right)^{n-1} \frac{\|c\| \left(\rho + \|A^{-1}\xi\| \right)}{|c^T A^{-1} \xi|} \right] \tag{20}$$

where

$$Re\left(\lambda(A)\right) \leq \gamma < 0 \tag{21}$$

$$\|A\| \leq M \tag{22}$$

$$0 < \epsilon < \min(2M, |\gamma|) \tag{23}$$

Proof: The explicit solution for y yields

$$y(t) = c^T e^{At} \left(x_0 + A^{-1}\xi \right) - c^T A^{-1} \xi \tag{24}$$

so $\hat{t}(x_0)$ is such that

$$c^T e^{A\hat{t}} \left(x_0 + A^{-1}\xi \right) = c^T A^{-1} \xi \tag{25}$$

that in turn implies

$$|c^T e^{A\hat{t}} \left(x_0 + A^{-1}\xi \right)| = |c^T A^{-1} \xi| \tag{26}$$

Moreover,

$$|c^T e^{A\hat{t}} \left(x_0 + A^{-1}\xi \right)| \leq \tag{27}$$

$$\|c\| \left(\frac{2M}{\epsilon} \right)^{n-1} e^{(\gamma+\epsilon)\hat{t}} \left(\|x_0 + A^{-1}\xi\| \right) \tag{28}$$

where we have used the estimate in [15, Proposition 3] for $\|e^{At}\|$. The statement of the Lemma follows by considering the worst case when x_0 varies in the ball of radius ρ. ∎

Lemma 1, with $c = e_1$, i.e., the vector with 1 as first entry and 0 elsewhere, produces the following estimate for the reaching time

$$\hat{t}_{reach} = \frac{1}{|\gamma + \epsilon|} \log \left[\left(\frac{2M}{\epsilon} \right)^{n-1} \frac{\left(\rho + \|A^{-1}\xi\| \right)}{|e_1^T A^{-1} \xi|} \right] \tag{29}$$

Remark 1: The estimate (29) is usually rather conservative and heavily depends on the selection of the parameters ϵ and M. It is possible to let $M = \|A\|$ and, noting that the term

$$\delta = \log \left[(2M)^{n-1} \frac{\left(\rho + \|A^{-1}\xi\| \right)}{|e_1^T A^{-1} \xi|} \right] \tag{30}$$

does not depend on ϵ, we can look for the value ϵ minimizing $\hat{t}_{reach}$ by solving the problem

$$\max_{\epsilon} \frac{1}{\gamma + \epsilon} \left(\delta + (1 - n) \log \epsilon \right) \tag{31}$$

with constraint (23). It is not hard, by computing the derivative of the (29), to show that the solution to (31) can be expressed as

$$\epsilon^* = \frac{\gamma}{W\left(\gamma e^{\frac{\delta}{n-1} - 1} \right)} \tag{32}$$

assuming ϵ^* satisfies (23), where $W(\cdot)$ is the *Lambert W function* defined by $z = W(ze^z)$ [16].

The results presented so far show how to design a control law such that the system state reaches a prescribed sliding manifold in finite time and stays on the manifold thereafter (at least in the hypothesis of ideal switching). This result can be used in two ways:

- If the battery has to be charged, a reference current $\bar{y}$ can be selected to be tracked by y;
- If the generator current must be limited to an upper bound I_{OL}, then, following the discussion at the end of Section II, a reference value $\bar{x}_2$ for x_2 is selected. In this case, k is obtained as [10]

$$k = \frac{-E_L \pm \sqrt{E_L^2 - 4R_L \bar{x}_2 (\alpha C_H \bar{x}_2 - E_H/R_H)}}{2R_L \bar{x}_2} \tag{33}$$

B. High-level control

From what has just been discussed it is clear that, when the battery has to be charged, it is sufficient to reach a sliding surface $\sigma = 0$ with k given by (11), while in the case of generator overload, in order to keep the generator current below an upper bound it is sufficient to choose k as in (33). The selection of the correct value for k is done by a supervisor. Thus, the supervisor has two modes, according to a known terminology used for hybrid systems [17], that are:

- Mode S1: active when the load energy demand is lower than the overload threshold and the constant k is

selected as in (11) in order to track a prescribed current to charge the battery.

- Mode S2: occurs when the load energy demand overcomes the generator current upper bound. This scenario implies a choice of k as in (33) such that the generator current is set to its upper bound. Thus, in turn, may result in two different cases: if the load requires less current than the overload threshold, then the generator charges the battery with less energy (reducing the current set point) than in nonoverload mode, otherwise the battery helps the generator supplying current to the high-voltage side. Both cases are handled automatically by Mode S2.

The commutation between the two modes is due to the change of load that causes the overload on the generator. The time instant when the load changes can be estimated by robust differentiation techniques (e.g., limited bandwidth differentiator, or Levant differentiator [18]). Moreover, in order to avoid chattering between the two modes, the commutation takes place with hysteresis on the generator current with band $[I_{OL} - \theta, I_{OL} + \theta]$. Note that in both modes the controller must adapt its action to the change of load. Specifically, stability of the control must be ensured both when the variation of the load causes a change of the supervisor mode and when the supervisor mode does not vary consequently to a change of the load.

Assume that the system is in steady mode with a given load R_{D1}. Next, suppose that, at a generic time instant t_k the load varies to a R_{D2} value so that the dynamic matrix A in (15) changes. Note that also the matrix B in (16) changes, and also the steady-state value changes. For this reason, we preliminary shift the steady-state at the origin with the change of variables

$$\zeta = z + A_i^{-1} B_i w, \quad i = 1, 2 \tag{34}$$

so that we have two LTI autonomous stable systems

$$\dot{\zeta} = A_1 \zeta \tag{35}$$

$$\dot{\zeta} = A_2 \zeta \tag{36}$$

It is well-known that if a CLF [19] can be found, then stability is not lost, irrespective of the commutation between the two systems. Looking for a CLF can be translated in solving the LMI problem

$$\begin{cases} A_1^T P + P A_1 < 0 \\ A_2^T P + P A_2 < 0 \\ P > 0 \end{cases} \tag{37}$$

where A_1 is the state matrix obtained when $R_D = R_{D1}$ while A_2 models the system when $R_D = R_{D2}$. Note that both matrices A_1 and A_2 are structured as in (15). Then, we can use $V(\zeta) = \zeta^T P \zeta$ as a CLF.

In general, this approach can be repeated for all loads (assuming a discrete set of possible loads, otherwise discretising the range of loads). However the search for a CLF is done only for systems of the form (14), i.e., for the reduced order systems. When switching among different reduced order systems we are sure that the state of the system, when observed from the metric of the CLF, can only decrease. In other words, defining $\chi = P^{1/2}\zeta$, we have $V = \|\chi\|^2$, that is always decreasing along the trajectories, since $\dot{V} < 0$. However, the actual commutation is not between two reduced system, and only when the reaching time has elapsed we are sure that the norm of the state reduces. Thus, before a further commutation is allowed to occur, we must ensure two conditions:

1) the reaching time has elapsed since the last commutation, so the system is surely on a sliding surface
2) the current state, when measured from the CLF metric, is not above the one just before the last commutation occurred.

The last condition is just a non-amplification condition, similar to the *monotonically nonincreasing* condition in [20, Definition 2.2]. Thus, the controller must not enable state transition lasting less than the reaching time and such that condition 2) is not satisfied.

Remark 2: In some cases, requiring the existence of a CLF can be too conservative. In this case it is possible to resort to less conservative approaches based on the combination of different Lyapunov functions and on Lyapunov-Metzler inequalities [21], [22]. This approach will be the subject of further research.

Remark 3: In the previous derivation we have supposed all the value of the parameters to be known. This may be acceptable for the network and BBCU parameters, but is unrealistic for the load, unless a feedforward solution is available. This issue is not considered in this paper, but has been considered in [10], where a Levant differentiator has been used to estimate both the time of change and the value of resistive load. Obviously, the time needed to estimate the load has to be added to the reaching time.

IV. Simulation Results

To test the proposed control strategy a MATLAB/Simulink/SimPowerSystem detailed simulator has been implemented as shown in Figure 2. The simulator presents six

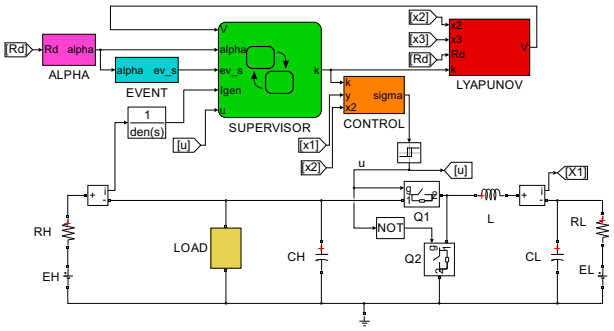

Fig. 2: Detailed Simulation Scheme

blocks, namely

- ALPHA: computes the value of α according to (5) (magenta block).
- EVENT: detects load variations (cyan block).

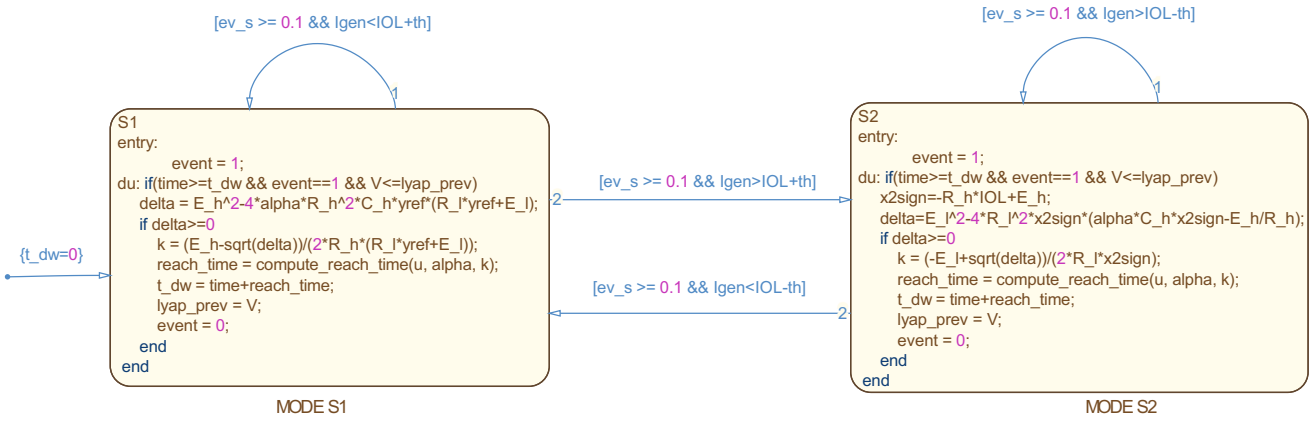

Fig. 3: Supervisor state flow

- SUPERVISOR: implements the supervisor logic (see Figure 3) and computes an estimate of the reaching time and k according to the current mode (green block).
- CONTROL: is the low-level control which implements the sliding mode control (orange block).
- LYAPUNOV: computes the Lyapunov function according to the reduced system state (red block).
- LOAD: contains a bank of three parallel resistors R_{Di} which can be individually connected to the circuit (yellow block).

The parameters considered in the simulations are shown in Tables Ia and Ib.

Parameter	Value	
E_L	28	[V]
E_H	270	[V]
L	10	[mH]
C_H	800	[μF]
C_L	400	[μF]
R_H	100	[mΩ]
R_L	100	[mΩ]
R_{D1}	300	[Ω]
R_{D2}	200	[Ω]
R_{D3}	16.5	[Ω]

(a) BBCU data

Name	Value	
I_{OL}	16	[A]
$\bar{y}$	10	[A]
θ	0.5	[A]

(b) Controller Parameter

TABLE I: Simulation parameters

The generator current detects the overload condition, thus, together with load changes, it is responsible for the transition between the two modes S1 and S2. Moreover, in order to remove the noise due to switching implementation it is filtered by a first-order transfer function

$$G(s) = \frac{1}{\tau_g s + 1}, \tag{38}$$

with $\tau_g = 0.01$s. Note that the filter is used only in the supervisor, and has no effect on the low-level control strategy.

At the beginning of the simulation, the supervisor is in mode S1 with load $R_D = R_{D1} = 300\Omega$ so the low-level goal is to control the inductor current y to $\bar{y} = 10A$. Figure 4 shows that starting from an initial value of $x_1(0) = 9$A, the inductor current reaches the reference value in short time.

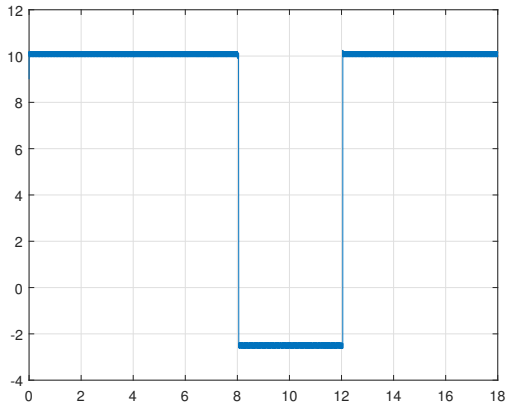

Fig. 4: Inductor current

At $t = 4$s the load changes to $R_D = R_{D2} = 200\Omega$. This variation of load causes a slight increase in the generator current (as apparent in Figure 5) which still remains below the overload threshold, therefore the supervisor remains in S1 mode and computes the reaching time and the updated k. At time instant $t = 8$s load is changed again to $R_D = R_{D3} = 16.5\Omega$. In this case the generator overload current is exceeded, thus the supervisor switches from mode S1 to S2, updates k and computes the reaching time which, in these particular conditions, is equal to 46ms. Note that during the reaching time interval the controller prevents any further variation of k, i.e., even in the case of further load changes the supervisor would not update k. After the reaching time has elapsed, the controller checks that the second condition in Section III-B is fulfilled before allowing a further update of mode or k. When in S2 mode, the low-level control objective is to drive the generator current to I_{OL}. Note that, as Figure 5 shows, the control goal is quickly reached thanks to the

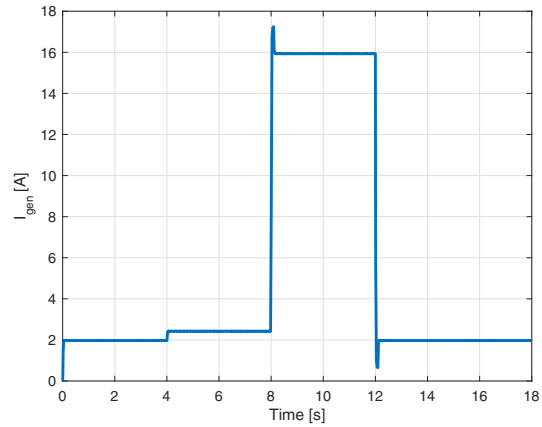

Fig. 5: Filtered generator current

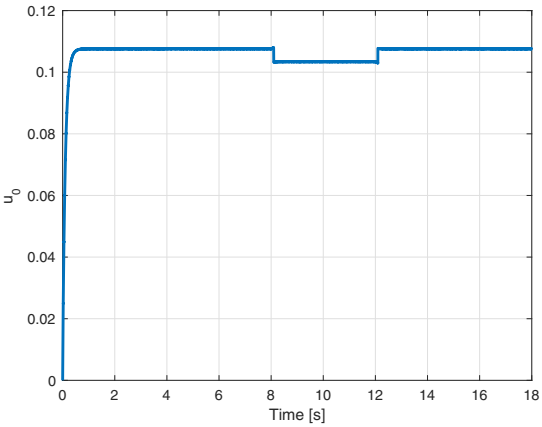

Fig. 6: Equivalent control

inductor current that assumes negative values as long as the load requires more current than the generator can supply. Finally, the load returns to its initial value and the controller automatically recovers the initial state of the closed-loop system.

Figure 6 shows that the equivalent control condition in (10) is satisfied. It is clear that in a more realistic version of the energy management system, also the battery state-of-charge should be taken into account. However, since only transient loads are considered in this paper, the "low-battery" event is not presented here.

V. CONCLUSIONS

An energy management system has been presented in this paper for advanced MEA applications. The focus was on battery charge in normal operations and on generator current limitation in the occurrence of an overload. A two-level control strategy is considered and mathematical proofs of stability are provided for both levels. Detailed simulations in the presence of different load scenarios are presented to show the effectiveness of the proposed approach. Further researches are devoted to on-line identification of loads and to management of state-of-charge of the battery.

REFERENCES

[1] J. Weimer, *Power management and distribution for the More Electric Aircraft*. American Society of Mechanical Engineers, New York, NY (United States), Dec 1995.

[2] M. A. Maldonado, N. M. Shah, K. J. Cleek, P. S. Walia, and G. Korba, "Power management and distribution system for a more-electric aircraft (madmel)-program status," in *IECEC 96. Proceedings of the 31st Intersociety Energy Conversion Engineering Conference*, vol. 1, Aug 1996, pp. 148–153 vol.1.

[3] B. Guida and A. Cavallo, "A petri net application for energy management in aeronautical networks," 2013.

[4] ——, "Supervised bidirectional dc/dc converter for intelligent fuel cell vehicles energy management," 2012.

[5] A. Cavallo, G. Canciello, and B. Guida, "Energy storage system control for energy management in advanced aeronautic applications," *Mathematical Problems in Engineering*, vol. 2017, 2017.

[6] I. Cotton, A. Nelms, and M. Husband, "Higher voltage aircraft power systems," *IEEE Aerospace and Electronic Systems Magazine*, vol. 23, no. 2, pp. 25–32, Feb 2008.

[7] P. Wheeler and S. Bozhko, "The more electric aircraft: Technology and challenges." *IEEE Electrification Magazine*, vol. 2, no. 4, pp. 6–12, Dec 2014.

[8] A. Cavallo and B. Guida, "Sliding mode control for dc/dc converters," in *Decision and Control (CDC), 2012 IEEE 51st Annual Conference on*, Dec 2012, pp. 7088–7094.

[9] B. Guida, L. Rubino, P. Marino, and A. Cavallo, "Implementation of control and protection logics for a bidirectional dc/dc converter," 2010, pp. 2696–2701.

[10] A. Cavallo, G. Canciello, and B. Guida, "Supervisory control of dc-dc bidirectional converter for advanced aeronautic applications," *International Journal of Robust and Nonlinear Control*, vol. 28, no. 1, pp. 1–15, 2018.

[11] ——, "Supervised control of buck-boost converters for aeronautical applications," *Automatica*, vol. 83, pp. 73–80, 2017.

[12] A. Cavallo, B. Guida, A. Buonanno, and E. Sparaco, "Smart buck-boost converter unit operations for aeronautical applications," in *2015 54th IEEE Conference on Decision and Control (CDC)*, Dec 2015, pp. 4734–4739.

[13] V. Utkin, J. Guldner, and J. Shi, *Sliding Mode Control in Electro-Mechanical Systems*. CRC Press, 2009.

[14] H. Sira-Ramirez, "Sliding motions in bilinear switched networks," *IEEE Trans. on Circuits and Systems*, vol. 34, pp. 919–933, 1987.

[15] W. Coppel, *Dichotomies in Stability Theory*, ser. Dichotomies in Stability Theory. Springer-Verlag, 1978, no. No. 629. [Online]. Available: https://books.google.it/books?id=cQBzDwEACAAJ

[16] R. M. Corless, G. H. Gonnet, D. E. G. Hare, D. J. Jeffrey, and D. E. Knuth, "On the lambertw function," *Advances in Computational Mathematics*, vol. 5, no. 1, pp. 329–359, Dec 1996. [Online]. Available: https://doi.org/10.1007/BF02124750

[17] R. Goebel, R. G. Sanfelice, and A. R. Teel, "Hybrid dynamical systems," *IEEE Control Systems*, vol. 29, no. 2, pp. 28–93, April 2009.

[18] A. Levant, "Robust exact differentiation via sliding mode technique," *Automatica*, vol. 34, no. 3, pp. 379 – 384, 1998.

[19] H. Lin and P. J. Antsaklis, "Stability and stabilizability of switched linear systems: A survey of recent results," *IEEE Transactions on Automatic Control*, vol. 54, no. 2, pp. 308–322, Feb 2009.

[20] M. S. Branicky, "Multiple lyapunov functions and other analysis tools for switched and hybrid systems," *IEEE Transactions on Automatic Control*, vol. 43, no. 4, pp. 475–482, Apr 1998.

[21] J. C. Geromel and P. Colaneri, "Stability and stabilization of continuous-time switched linear systems," *SIAM Journal on Control and Optimization*, vol. 45, no. 5, pp. 1915–1930, 2006. [Online]. Available: https://doi.org/10.1137/050646366

[22] G. Chesi, P. Colaneri, J. C. Geromel, R. Middleton, and R. Shorten, "A nonconservative lmi condition for stability of switched systems with guaranteed dwell time," *IEEE Transactions on Automatic Control*, vol. 57, no. 5, pp. 1297–1302, May 2012.